Next-to-leading order corrections to top quark decays to heavy quarkonia

Peng Sun,[1] Li-Ping Sun,[1] and Cong-Feng Qiao[1,2,*]

[1]*College of Physical Sciences, Graduate University of Chinese Academy of Sciences, YuQuan Road 19A, Beijing 100049, China*
[2]*Theoretical Physics Center for Science Facilities (TPCSF), Chinese Academy of Science, YuQuan Road 19B, Beijing 100049, China*
(Received 2 April 2010; published 24 June 2010)

The decay widths of top quark to S-wave $b\bar{c}$ and $b\bar{b}$ bound states are evaluated at the next-to-leading-order accuracy in strong interaction. Numerical calculation shows that the next-to-leading-order corrections to these processes are remarkable. The QCD renormalization scale dependence of the results is obviously depressed, and hence the uncertainties lying in the leading order calculation are reduced.

DOI: 10.1103/PhysRevD.81.114035 PACS numbers: 13.85.Ni, 12.38.Bx, 12.39.Hg, 14.40.Nd

I. INTRODUCTION

Since predicted by the standard model [1–3], top quark has become an important role in high energy physics due to its large mass, which is close to the electroweak symmetry breaking scale [4]. A great deal of research focusing on top quark physics have been performed after its discovery in 1995 in the Fermilab [5]. Regarding the experiment aspect, with the running of the Tevatron and forthcoming LHC, the lack of adequate events will not be an obstacle for the top quark physics study. According to Ref. [6], at the LHC $10^7 \sim 10^8$ $t\bar{t}$ pairs can be obtained per year, so this enables the measurement of various top quark decay channels. Meanwhile, the copious production of the top quarks also produces a great number of bottom quark mesons since the dominant top quark decay channel is $t \to b + W^+$. Therefore, the bottom quark meson production in top quark decays may stand as an important and independent means for the study of heavy meson physics and the test of perturbative QCD (pQCD).

As the known heaviest mesons, bottomonia and B_c ($b\bar{c}$ or $\bar{b}c$) possess particular meaning in the study of heavy flavor physics. The LHCb as a detector specifically for the heavy flavor study at the LHC will supply copious B_c and Υ data for this aim. Theoretically, the direct hadro production of B_c and Υ was studied in the literature [7–9]. In addition to the ''direct'' production, ''indirect'' process as in top quark decays may stand as an independent and important source for B_c and Υ production. Since the top quark's lifetime is too short to form a bound state [10], the B_c and Υ production involved scheme in top quark decays is less affected by the nonpertubative effects than in other processes. In Ref. [11], the top quark decays into Υ and $\bar{B}_c^*$ at the Born level was evaluated. Recently, the S- and P-wave B_c meson productions in top quark decays were fully evaluated, including the color-octet contributions, at the leading order accuracy of QCD by Chang *et al.* [12].

Considering the importance of investigating B_c and Υ in the study of pQCD and potential models, it is reasonable and interesting to evaluate the production rates of these mesons in top quark decays at the next-to-leading order (NLO) accuracy of pQCD. At the bottom quark and charm quark mass scales the strong coupling is not very small; therefore, the higher order corrections are usually large. On the other hand, in the processes of top quark decays into $\bar{B}_c(\Upsilon)$, the $t \to b\bar{c}(\bar{b}) + c(b) + W^+$, there exist large scale uncertainties in the tree level calculation [13]. The NLO corrections should in principle minimize it and give a more precise prediction. To calculate the $\bar{B}_c$ and Υ production rates in top quark decays at the NLO accuracy are the aims of this work. In our calculation, both of the S-wave spin-singlet and -triplet states are taken into account, i.e., $\bar{B}_c^*$, $\bar{B}_c$, Υ, and η_b. To deal with the nonperturbative effects, the nonrelativistic QCD [14] effective theory is employed. The calculation will be performed at the NLO in pQCD expansion, but at leading order in relativistic expansion, that is, in the expansion of v, the relativistic velocity of heavy quarks inside bound states.

The paper is organized as follows: after the Introduction, in Sec. II we explain the calculation of leading order decay width. In Sec. III, virtual and real QCD corrections to the Born level result are evaluated. In Sec. IV, the numerical calculation for concerned processes at the NLO accuracy of pQCD is performed, and the scale dependence of the results is shown. The last remaining section provides a brief summary and our conclusions.

II. CALCULATION OF THE BORN LEVEL DECAY WIDTH

At the leading order in α_s, there are two Feynman diagrams for each meson production, which are shown in Fig. 1. For the convenience of analytical calculation, taking $\bar{B}_c$ as an example, the momentum of each particle is assigned as $p_1 = p_t$, $p_3 = p_b$, $p_4 = p_{\bar{c}}$, $p_5 = p_c$, $p_6 = p_{W^+}$, $p_0 = p_3 + p_4$, $p_3 = \frac{m_b}{m_c} p_4$. For bottomonium, the only difference is that p_4 and p_5 represent the momenta of antibottom quark and bottom quark, which are produced in gluon splitting.

Of the $\bar{B}_c$ and $\bar{B}_c^*$ production in top quark decays, i.e.,

$$t(p_1) \to \bar{B}_c/\bar{B}_c^*(p_0) + c(p_5) + W^+(p_6), \qquad (1)$$

*Corresponding author, qiaocf@gucas.ac.cn

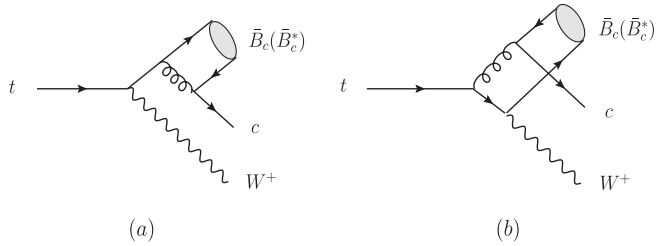

FIG. 1. The leading order Feynman diagrams for $\bar{B}_c$ and $\bar{B}_c^*$ production in top quark decays.

we employ the following commonly used projection operators for quarks hadronization

$$v(p_4)\bar{u}(p_3) \to \frac{1}{2\sqrt{2}} i\gamma_5(\not{p}_0 + m_b + m_c) \times \left(\frac{1}{\sqrt{\frac{m_b+m_c}{2}}}\psi_{\bar{B}_c}(0)\right) \otimes \left(\frac{\mathbf{1}_c}{\sqrt{N_c}}\right) \quad (2)$$

and

$$v(p_4)\bar{u}(p_3) \to \frac{1}{2\sqrt{2}} \not{\varepsilon}_{\bar{B}_c^*}(\not{p}_0 + m_b + m_c) \times \left(\frac{1}{\sqrt{\frac{m_b+m_c}{2}}}\psi_{\bar{B}_c^*}(0)\right) \otimes \left(\frac{\mathbf{1}_c}{\sqrt{N_c}}\right). \quad (3)$$

Here, $\varepsilon_{\bar{B}_c^*}$ is the polarization vector of $\bar{B}_c^*$ with $p_0 \cdot \varepsilon = 0$, $\mathbf{1}_c$ stands for the unit color matrix, and $N_c = 3$ for QCD. The nonperturbative parameters $\psi_{\bar{B}_c}(0)$ and $\psi_{\bar{B}_c^*}(0)$ are the Schrödinger wave functions at the origin of $b\bar{c}$ bound states, and in the nonrelativistic limit $\psi_{\bar{B}_c}(0) = \psi_{\bar{B}_c^*}(0)$. In our calculation, the nonrelativistic relation $m_{\bar{B}_c} = m_{\bar{B}_c^*} = m_b + m_c$ is also adopted.

The LO amplitudes for $\bar{B}_c$ production can then be readily obtained with above preparations. They are

$$\mathcal{M}_a = \frac{\pi\alpha_s g \psi_{\bar{B}_c}(0) V_{tb} C_F \delta_{j,k}}{\sqrt{6m_{\bar{B}_c}}} \bar{u}(p_5)\gamma^\mu i\gamma_5(\not{p}_0 + m_{\bar{B}_c})\gamma_\mu \times \frac{(\not{p}_0 + \not{p}_5 + m_b)}{(p_0 + p_5)^2 - m_b^2} \frac{\not{\epsilon}(p_6)(1-\gamma_5)}{(p_4 + p_5)^2} u(p_1), \quad (4)$$

and

$$\mathcal{M}_b = \frac{\pi\alpha_s g \psi_{\bar{B}_c}(0) V_{tb} C_F \delta_{j,k}}{\sqrt{6m_{\bar{B}_c}}} \bar{u}(p_5)\gamma^\mu i\gamma_5(\not{p}_0 + m_{\bar{B}_c}) \times \frac{\not{\epsilon}(p_6)(1-\gamma_5)}{(p_4 + p_5)^2} \frac{(\not{p}_3 + \not{p}_6 + m_t)}{(p_3 + p_6)^2 - m_t^2} \gamma_\mu u(p_1). \quad (5)$$

Here, j, k are color indices, $C_F = 4/3$ belongs to the $SU(3)$ color structure. For $\bar{B}_c^*$ production, the amplitudes can be obtained by simply substituting $i\gamma_5(\not{p}_0 + m_{\bar{B}_c})$ with $\not{\epsilon}_{\bar{B}_c^*}(\not{p}_0 + m_b + m_c)$ in the above expressions.

The Born amplitude of the processes shown in Fig. 1 is then $\mathcal{M}_{\text{Born}} = \mathcal{M}_a + \mathcal{M}_b$, and subsequently, the decay width at leading order reads

$$d\Gamma_{\text{Born}} = \frac{1}{2m_t}\frac{1}{2}\frac{1}{N_c}\sum |\mathcal{M}_{\text{Born}}|^2 \text{dPS}_3. \quad (6)$$

Here, $\sum$ represents the sum over polarizations and colors of the initial and final particles, $\frac{1}{2}$ and $\frac{1}{N_c}$ come from spin and color average of initial top quark, dPS_3 stands for the integrands of three-body phase space, whose concrete form is

$$\text{dPS}_3 = \frac{1}{32\pi^3}\frac{1}{4m_t^2} ds_1 ds_2, \quad (7)$$

where $s_1 = (p_0 + p_5)^2 = (p_1 - p_6)^2$ and $s_2 = (p_5 + p_6)^2 = (p_1 - p_0)^2$ are Mandelstam variables. The upper and lower bounds of the above integration are

$$s_1^{\max} = \frac{\sqrt{f[m_t^2, s_2, m_{\bar{B}_c}^2] \cdot f[s_2, m_c^2, m_W^2]} + [m_t^2 - s_2 - (m_b + m_c)^2](s_2 + m_c^2 - m_W^2)}{2s_2} + m_{\bar{B}_c}^2 + m_c^2, \quad (8)$$

$$s_1^{\min} = -\frac{\sqrt{f[m_t^2, s_2, m_{\bar{B}_c}^2] \cdot f[s_2, m_c^2, m_W^2]} - [m_t^2 - s_2 - (m_b + m_c)^2](s_2 + m_c^2 - m_W^2)}{2s_2} + m_{\bar{B}_c}^2 + m_c^2, \quad (9)$$

and

$$s_2^{\max} = [m_t - (m_b + m_c)]^2, \qquad s_2^{\min} = (m_c + m_W)^2, \quad (10)$$

with

$$f[x, y, z] = (x - y - z)^2 - 4yz. \quad (11)$$

III. THE NEXT-TO-LEADING ORDER CORRECTIONS

At the next-to-leading order, the top quark decays to $\bar{B}_c$ and Υ include the virtual and real QCD corrections to the leading order process, as shown in Figs. 2–5. With virtual corrections, the decay widths at the NLO can be formulated as

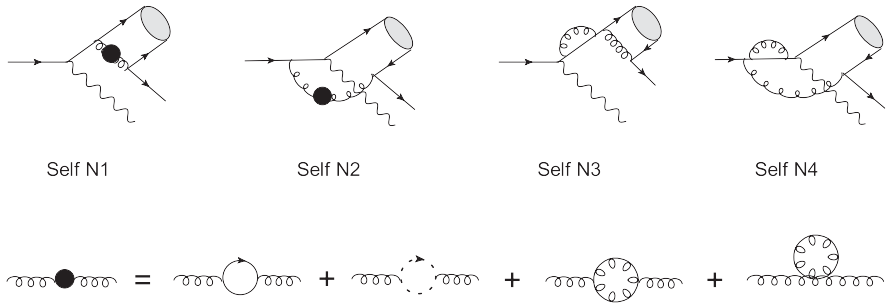

FIG. 2. The self-energy diagrams in virtual corrections.

$$d\Gamma_{\text{Virtual}} = \frac{1}{2m_t}\frac{1}{2}\frac{1}{N_c}\sum 2\,\text{Re}(\mathcal{M}^*_{\text{Born}}\mathcal{M}_{\text{Virtual}})\text{dPS}_3. \quad (12)$$

The ultraviolet (UV) and infrared (IR) divergences usually exist in virtual corrections. We use the dimensional regularization scheme to regularize the UV and IR divergences, similar as performed in Ref. [15], and the Coulomb divergence is regularized by the relative velocity v. In dimensional regularization, γ_5 is difficult to deal with. In this calculation, we adopt the naive scheme, that is, γ_5 anticommutates with each γ^μ matrix in d-dimension spacetime, $\{\gamma_5, \gamma^\mu\} = 0$. The UV divergences exist merely in self-energy and triangle diagrams, which can be renormalized by counter terms. The renormalization constants include Z_2, Z_3, Z_m, and Z_g, corresponding to quark field, gluon field, quark mass, and strong coupling constant α_s, respectively. Here, in our calculation the Z_g is defined in the modified-minimal-subtraction ($\overline{\text{MS}}$) scheme, while for the other three the on-shell (OS) scheme is adopted, which tells

$$\begin{aligned}
\delta Z_m^{\text{OS}} &= -3C_F\frac{\alpha_s}{4\pi}\left[\frac{1}{\epsilon_{\text{UV}}} - \gamma_E + \ln\frac{4\pi\mu^2}{m^2} + \frac{4}{3} + \mathcal{O}(\epsilon)\right],\\
\delta Z_2^{\text{OS}} &= -C_F\frac{\alpha_s}{4\pi}\left[\frac{1}{\epsilon_{\text{UV}}} + \frac{2}{\epsilon_{\text{IR}}} - 3\gamma_E + 3\ln\frac{4\pi\mu^2}{m^2}\right.\\
&\quad \left. + 4 + \mathcal{O}(\epsilon)\right],\\
\delta Z_3^{\text{OS}} &= \frac{\alpha_s}{4\pi}\left[(\beta_0 - 2C_A)\left(\frac{1}{\epsilon_{\text{UV}}} - \frac{1}{\epsilon_{\text{IR}}}\right) + \mathcal{O}(\epsilon)\right],\\
\delta Z_g^{\overline{\text{MS}}} &= -\frac{\beta_0}{2}\frac{\alpha_s}{4\pi}\left[\frac{1}{\epsilon_{\text{UV}}} - \gamma_E + \ln 4\pi + \mathcal{O}(\epsilon)\right].
\end{aligned} \quad (13)$$

Here, $\beta_0 = (11/3)C_A - (4/3)T_f n_f$ is the one-loop coefficient of the QCD beta function; $n_f = 5$ is the number of active quarks in our calculation; $C_A = 3$ and $T_F = 1/2$ attribute to the $SU(3)$ group; μ is the renormalization scale.

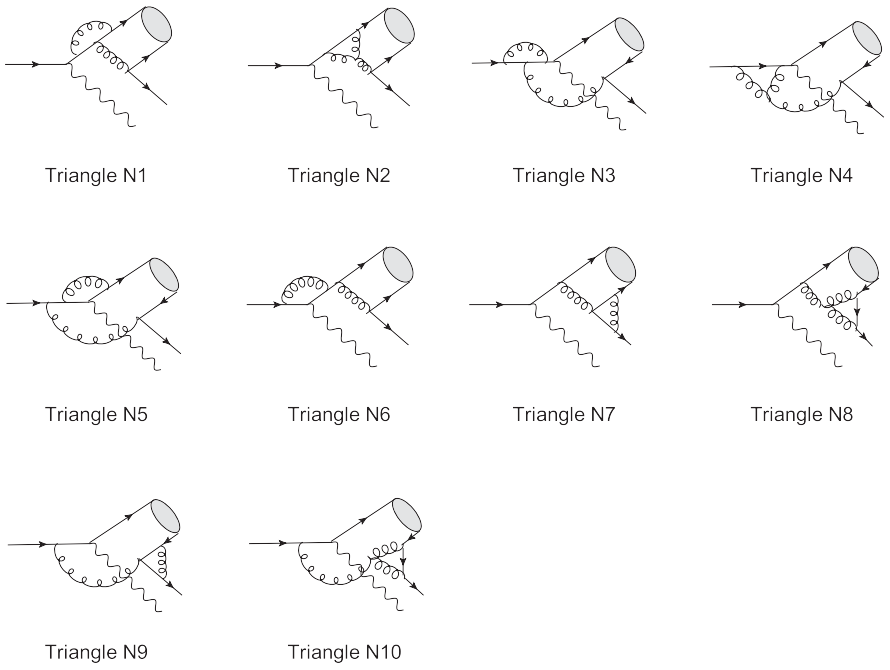

FIG. 3. The triangle diagrams in virtual corrections.

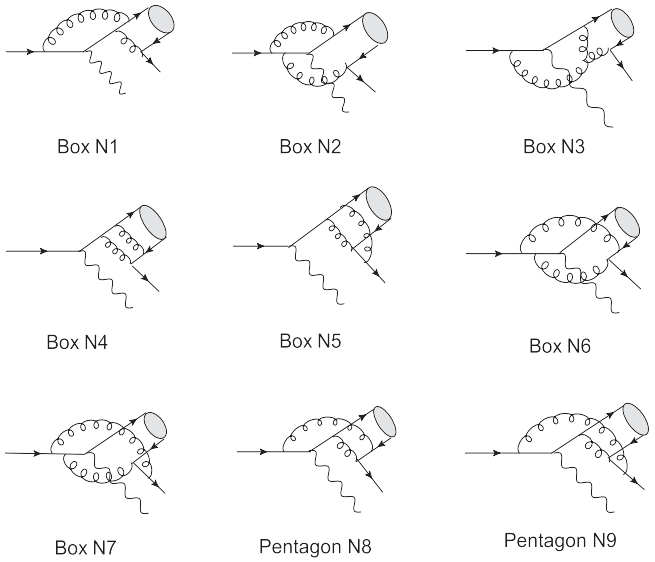

FIG. 4. The box and pentagon diagrams in virtual corrections.

In virtual corrections, IR divergences remain in the triangle and box diagrams. Of all the triangle diagrams, only two have IR divergences, which are denoted as TriangleN7 and TriangleN9 in Fig. 3. Of the diagrams in Fig. 4, BoxN3 has no IR singularity, while BoxN4 and PentagonN9 have Coulomb singularities and PentagonN9 possesses ordinary IR singularity as well. The remaining diagrams all have IR singularities, while the combinations BoxN2+BoxN6, BoxN1+PentagonN8+TriangleN9, BoxN5+TriangleN7 are IR finite. The Coulomb singularities belonging to BoxN4 and PentagonN9 can be regularized by the relative velocity v. After regularization procedure, the $\frac{1}{\epsilon}$ term will be canceled out by the counter terms of external quarks which form the $\bar{B}_c$ or Υ, while the $\frac{1}{v}$ term will be mapped onto the wave functions of the concerned heavy mesons. The remaining IR singularities in BoxN7 and BoxN9 are canceled by the corresponding parts in real corrections. In the end, the IR and Coulomb divergences in virtual corrections can be expressed as

$$d\Gamma^{\mathrm{IR,Coulomb}}_{\mathrm{virtual}} = d\Gamma_{\mathrm{Born}} \frac{4\alpha_s}{3\pi}\left[\frac{\pi^2}{v} - \frac{1}{\epsilon} - \frac{p_t \cdot p_c x_s \ln x_s}{m_c m_t (1-x_s^2)} \frac{1}{\epsilon}\right], \tag{14}$$

with $p_t = p_1$, $p_c = p_5$ and $x_s = \frac{1-\sqrt{1-2m_c m_t/(m_c m_t - p_t\cdot p_c)}}{1+\sqrt{1-2m_c m_t/(m_c m_t - p_t\cdot p_c)}}$. Here, in this work $\frac{1}{\epsilon}$ in fact represents $\frac{1}{\epsilon} - \gamma_E + \ln(4\pi\mu^2)$.

Of our concerned processes, there are 12 different diagrams in real corrections, as shown in Fig. 5. Among them, RealN2, RealN3, RealN8, and RealN9 are IR finite, meanwhile the combinations of RealN1+RealN5 and RealN10+RealN11 exibit no IR singularities as well, due to the reasons of gluon connecting to the b or $\bar{c}$ quark of final $\bar{B}_c$ or Υ. The remaining diagrams, RealN4, RealN6, RealN7, and RealN12 are not IR singularity free. To regularize the IR divergence, we enforce a cut on the gluon momentum, the p_7. The gluon with energy $p_7^0 < \delta$ is considered to be soft, while $p_7^0 > \delta$ is thought to be hard. The δ is a small quantity with energy-momentum unit. In this case, the IR term of the decay width can then be written as

$$d\Gamma^{\mathrm{IR}}_{\mathrm{Real}} = \frac{1}{2m_t}\frac{1}{2}\frac{1}{N_c}\sum |\mathcal{M}_{\mathrm{Real}}|^2 \mathrm{dPS}_4|_{\mathrm{soft}}, \tag{15}$$

where dPS_4 is the four-body phase space integrands for real corrections. Under the condition of $p_7^0 < \delta$, in the Eikonal approximation we obtain

$$\mathrm{dPS}_4|_{\mathrm{soft}} = \mathrm{dPS}_3 \frac{d^3 p_7}{(2\pi)^3 2p_7^0}|_{p_7^0<\delta} \tag{16}$$

In the small δ limit, the IR divergent terms in real correc-

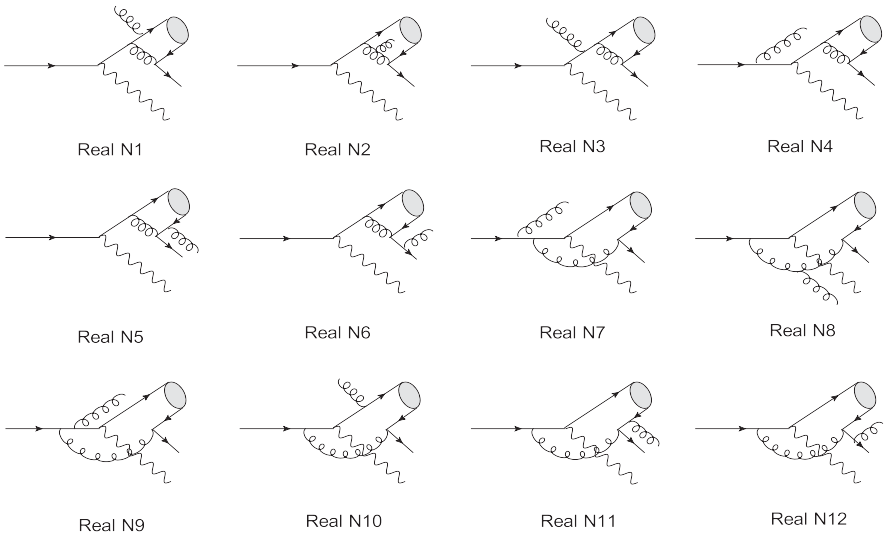

FIG. 5. The real correction Feynman diagrams that contribute to the production of $\bar{B}_c$ or $\bar{B}_c^*$.

tion can therefore be expressed as

$$d\Gamma_{\rm Real}^{\rm IR} = d\Gamma_{\rm Born}\frac{4\alpha_s}{3\pi}\left\{\left(\frac{1}{\epsilon}-{\rm Log}(\delta^2)\right)\left[1+\frac{p_t\cdot p_c x_s \ln x_s}{m_c m_t(1-x_s^2)}\right] + \text{ finite terms}\right\}. \quad (17)$$

Here, the $\mathrm{Log}(\delta^2)$ involved terms will be canceled out by the δ-dependent terms in the hard sector of real corrections. Referring to Eq. (14), it is obvious that the IR divergent terms in real and virtual corrections cancel each other. In case of hard gluons in real correction, the decay width reads

$$d\Gamma_{\rm Real}^{\rm hard} = \frac{1}{2m_t}\frac{1}{2}\frac{1}{N_c}\sum|\mathcal{M}_{\rm Real}|^2 {\rm dPS}_4|_{\rm hard}. \quad (18)$$

In this case, the phase space $\mathrm{dPS}_4|_{\rm hard}$ can be written as

$$\begin{aligned}{\rm dPS}_4|_{\rm hard} = {}& \frac{2}{(4\pi)^6}\frac{\sqrt{(sy+m_c^2-m_W^2)^2-4sym_c^2}}{y}\int_{p_{0-}^0}^{p_{0+}^0}dp_0^0 \\ & \times\int_{-1}^{1}d\cos\theta_c\int_0^{2\pi}d\phi_c\times\left\{\int_{\delta}^{p_{7-}^0}dp_7^0\int_{y_-}^{y_+}dy \right. \\ & \left. +\int_{p_{7-}^0}^{p_{7+}^0}dp_7^0\int_{((m_c+m_W)^2/s)}^{y_+}dy\right\}, \end{aligned} \quad (19)$$

with

$${p_{0-}}^0 = m_b + m_c, \quad (20)$$

$${p_{0+}}^0 = \frac{s+m_b^2-m_W^2+2m_bm_c-2m_W\cdot m_c}{2\sqrt{s}}, \quad (21)$$

$${p_{7-}}^0 = \frac{s+m_b^2-m_W^2+2m_bm_c-2m_W\cdot m_c-2\sqrt{s}{p_0}^0}{2\sqrt{s}-2{p_0}^0+2\sqrt{|\vec{p}_0|}}, \quad (22)$$

$${p_{7+}}^0 = \frac{s+m_b^2-m_W^2+2m_bm_c-2m_W\cdot m_c-2\sqrt{s}{p_0}^0}{2\sqrt{s}-2{p_0}^0-2\sqrt{|\vec{p}_0|}}, \quad (23)$$

$$y_- = \frac{1}{s}[(\sqrt{s}-{p_0}^0-{p_7}^0)^2-|\vec{p}_0|^2-({p_7}^0)^2-2|\vec{p}_0|p_7^0], \quad (24)$$

$$y_+ = \frac{1}{s}[(\sqrt{s}-{p_0}^0-{p_7}^0)^2-|\vec{p}_0|^2-({p_7}^0)^2+2|\vec{p}_0|{p_7}^0], \quad (25)$$

where y is a dimensionless parameter defined as $y=(p_1-p_0-p_7)^2/s$ with $\sqrt{s}=m_t$, and

$$|\vec{p}_0| = \sqrt{({p_0}^0)^2-m_{\bar{B}_c}^2}. \quad (26)$$

The sum of the soft and hard sectors gives the total contribution of real corrections, i.e., $\Gamma_{\rm Real}=\Gamma_{\rm Real}^{\rm IR}+\Gamma_{\rm Real}^{\rm hard}$.

With the real and virtual corrections, we then obtain the total decay width of top quark to $\bar{B}_c$ and Υ at the NLO accuracy of QCD

$$\Gamma_{\rm total} = \Gamma_{\rm Born}+\Gamma_{\rm Virtual}+\Gamma_{\rm Real}+\mathcal{O}(\alpha_s^4). \quad (27)$$

In above expression, the decay width is UV and IR finite. In our calculation the FEYNARTS [16] was used to generate the Feynman diagrams, the amplitudes were generated by the FEYNCALC [17], and the LOOPTOOLS [18] was employed to calculate the Passarino-Veltman integrations. The numerical integrations of the phase space were performed by the MATHEMATICA.

IV. NUMERICAL RESULTS

To complete the numerical calculation, the following ordinarily accepted input parameters are taken into account:

$$\begin{aligned} m_b &= 4.9\ \text{GeV}, & m_c &= 1.5\ \text{GeV}, \\ m_t &= 174\ \text{GeV}, & m_W &= 80\ \text{GeV}, \end{aligned} \quad (28)$$

$$\psi_{\bar{B}_c}(0) = \psi_{\bar{B}_c^*}(0) = \frac{R_1(0)}{\sqrt{4\pi}} = 0.3616\ \text{GeV}^{3/2}, \quad (29)$$

$$\psi_\Upsilon^{\rm LO}(0) = \psi_{\eta_b}^{\rm LO}(0) = \frac{R_2^{\rm LO}(0)}{\sqrt{4\pi}} = 0.6812\ \text{GeV}^{3/2}, \quad (30)$$

$$\psi_\Upsilon^{\rm NLO}(0) = \psi_{\eta_b}^{\rm NLO}(0) = \frac{R_2^{\rm NLO}(0)}{\sqrt{4\pi}} = \frac{R_2^{\rm LO}(0)}{\sqrt{4\pi-16C_F\alpha_s}} = 0.8277\ \text{GeV}^{3/2}, \quad (31)$$

$$V_{tb} = 1.0, \qquad G_F = 1.1660\times10^{-5}\ \text{GeV}^{-2}. \quad (32)$$

Here, V_{tb} is the Cabibbo-Kobayashi-Maskawa matrix element and G_F is weak interaction Fermi constant.

In above numerical calculation inputs, the radial wave function at the origin for S-wave $\bar{B}_c^*(\bar{B}_c)$ system is estimated by potential models [19], while the corresponding $\Upsilon(\eta_b)$ nonperturbative parameter is determined from its electronic decay rate [8]. A one-loop result of strong coupling constant is taken into account, i.e.,

$$\alpha_s(\mu) = \frac{4\pi}{(11-\frac{2}{3}n_f)\mathrm{Log}(\frac{\mu^2}{\Lambda_{\rm QCD}^2})}. \quad (33)$$

With the above preparation, one can readily obtain the decay widths of top quark to $b\bar{c}$ and $b\bar{b}$ mesons, as listed in Table I. To see the scale dependence of the LO and NLO results, the ratios $\Gamma(\mu)/\Gamma(2m_c)$ for $b\bar{c}$ system and $\Gamma(\mu)/\Gamma(2m_b)$ for $b\bar{b}$ system are showed in Figs. 6 and 7, respectively. Our calculation tells us that after including

TABLE I. The decay widths of the processes $t \to \bar{B}_c^* + W^+ + c$, $t \to \bar{B}_c + W^+ + c$, $t \to \Upsilon + W^+ + b$ and $t \to \eta_b + W^+ + b$ at the tree level and with the NLO QCD corrections are presented in two renormalization scale μ limits; those are $2m_c$ and m_t for the first two processes and $2m_b$ and m_t for the other two.

	$t \to \bar{B}_c^* + W^+ + c$		$t \to \bar{B}_c + W^+ + c$		$t \to \Upsilon + W^+ + b$		$t \to \eta_b + W^+ + b$	
μ	$2m_c$	m_t	$2m_c$	m_t	$2m_b$	m_t	$2m_b$	m_t
Γ_{LO}	0.793 MeV	0.151 MeV	0.572 MeV	0.109 MeV	26.8 keV	9.54 keV	27.1 keV	9.67 keV
Γ_{NLO}	0.619 MeV	0.307 MeV	0.514 MeV	0.227 MeV	52.3 keV	28.2 keV	34.3 keV	24.5 keV

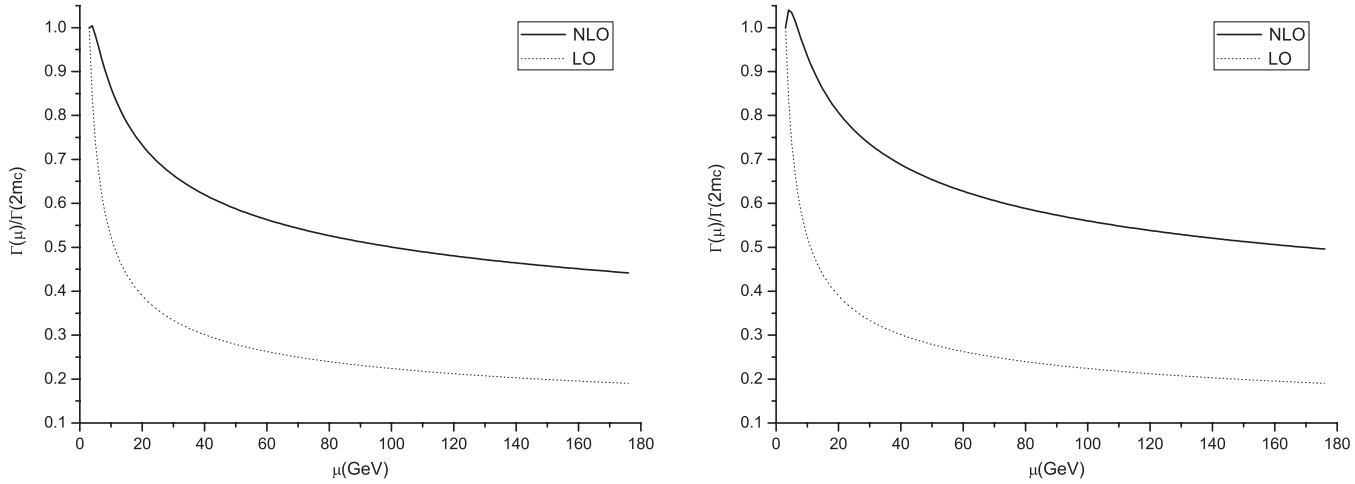

FIG. 6. The ratio $\Gamma(\mu)/\Gamma(2m_c)$ versus renormalization scale μ in top quark decays. The left diagram for the $b\bar{c}$ spin-singlet state $\bar{B}_c$ and the right diagram for the spin-triplet state $\bar{B}_c^*$.

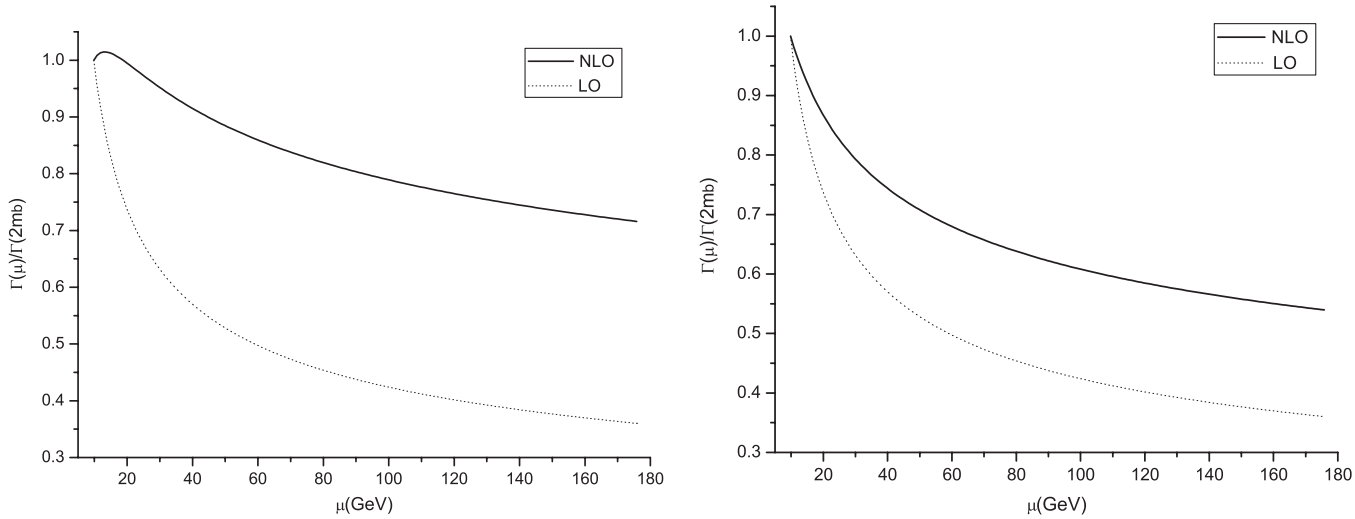

FIG. 7. The ratio $\Gamma(\mu)/\Gamma(2m_b)$ versus renormalization scale μ in top quark decays. The left diagram for the $b\bar{b}$ spin-singlet state η_b and the right diagram for the spin-triplet state Υ.

the NLO corrections, the energy scale dependence of the results is reduced, as expected.

V. SUMMARY AND CONCLUSIONS

In this work we have calculated the decay widths of top quark to S-wave $b\bar{c}$ and $b\bar{b}$ bound states at the NLO accuracy of perturbative QCD. Considering that there will be copious $t\bar{t}$ data in the near future at the LHC, our results are helpful to the study of the indirect production of these states. They may be also useful to the future study of NLO heavy quark to $b\bar{c}$ and $b\bar{b}$ bound states fragmentation functions.

Numerical results indicate that the NLO corrections greatly enhance the LO results for the $b\bar{b}$ system, while slightly decreasing the $b\bar{c}$ states' production widths. The main reason for this difference is that the NLO wave function for bottomonium is much larger than that of the LO one, while for the calculation of the $\bar{B}_c$ meson, the same wave function given by potential models is used. Although from Table I, superficially the number of indirectly produced $\bar{B}_c$ overshoots that of Υ, experimentally to detect the latter is much easier than the former. Since top quark dominantly decays into a b and W^+ final state with a width of 1.5 GeV or so, numerical results remind us that the Υ indirect production from top quark decay is detectable, while it is hard to pin down the $\bar{B}_c$ states by this way.

The numerical calculation also shows that the next-to-leading order QCD corrections to processes $t \to b\bar{c}(b\bar{b}) + W^+ + c(b)$ decrease the energy scale dependence of the decay widths as expected, and hence the uncertainties in theoretical estimation. Future precise experiment on the concerned processes may provide a test on the theoretical framework for heavy quarkonium production and the reliability of perturbative calculation for them.

ACKNOWLEDGMENTS

This work was supported in part by the National Natural Science Foundation of China (NSFC) under the Grant Nos. 10935012, 10928510, 10821063, and 10775179, by the CAS Key Project Nos. KJCX2-yw-N29, and H92A0200S2.

[1] W. Hollik, in *Proceedings of the XVI International Symposium on Lepton-Photon Interactions* (Cornell University, Ithaca, NY, 1993); M. Swartz, in *Proceedings of the XVI International Symposium on Lepton-Photon Interactions* (Cornell University, Ithaca, NY, 1993).

[2] G. Altarelli, in *International University School of Nuclear and Particle Physics, 32nd: Substructures of Matter as Revealed with Electroweak Probes, Schladaing, Austria, Feb 24–Mar 5, 1993*, edited by L. Mathelitsch and W. Plessas (Springer-Verlag, Berlin, 1994).Lect. Notes Phys., **426**, 441 (1993).

[3] G. Altarelli, in *1st International Conference on Phenomenology of Unification: From Present to Future, Rome, 1994* (CERN Report No. CERN-TH-7319/94 1994).

[4] G. L. Kane, in *Proceedings of the Workshop on High Energy Phenomenology, Mexico City, Jul 1–12, 1991*, edited by M. A. Perez and R. Huerta (World Scientific, Singapore, 1992).

[5] F. Abe *et al.* (CDF Collaboration), Phys. Rev. Lett. **74**, 2626 (1995); S. Abachi *et al.* (D0 Collaboration), Phys. Rev. Lett. **74**, 2632 (1995).

[6] N. Kidonakis and R. Vogt, Int. J. Mod. Phys. A **20**, 3171 (2005); F. Hubaut *et al.* (ATLAS Collaboration), arXiv: hep-ex/0605029; V. Barger and R. J. Phillips, Report No. MAD/PH/789, 1993.

[7] E. Braaten and T. C. Yuan, Phys. Rev. Lett. **71**, 1673 (1993); Phys. Rev. D **50**, 3176 (1994); C.-H. Chang and Y.-Q. Chen, Phys. Lett. B **284**, 127 (1992); Phys. Rev. D **46**, 3845 (1992); Y.-Q. Chen, Phys. Rev. D **48**, 5181 (1993); T. C. Yuan, Phys. Rev. D **50**, 5664 (1994).

[8] E. Braaten, K. Cheung, and T. C. Yuan, Phys. Rev. D **48**, 4230 (1993); **48**, R5049 (1993).

[9] K. Kolodzidj, A. Leike, and R. Ruckl, Phys. Lett. B **355**, 337 (1995); C.-H. Chang and Y.-Q. Chen, Phys. Lett. B **364**, 78 (1995); Phys. Rev. D **48**, 4086 (1993); C.-H. Chang, Int. J. Mod. Phys. A **21**, 777 (2006); C.-H. Chang, J.-X. Wang, and X.-G. Wu, Phys. Rev. D **70**, 114019 (2004); C.-H. Chang, C.-F. Qiao, J. X. Wang, and X.-G. Wu, Phys. Rev. D **71**, 074012 (2005); C.-H. Chang and X.-G. Wu, Eur. Phys. J. C **38**, 267 (2004); C.-H. Chang, C. Driouichi, P. Eerola, and X.-G. Wu, Comput. Phys. Commun. **159**, 192 (2004); C.-H. Chang, J.-X. Wang, and X.-G. Wu, Comput. Phys. Commun. **174**, 241 (2006).

[10] I. I. Bigi, Y. L. Dokshitzer, V. A. Khoze, J. H. Kuhn, and P. Zerwas, Phys. Lett. B **181**, 157 (1986); L. H. Orr and J. L. Rosner, Phys. Lett. B **246**, 221 (1990).

[11] C.-F. Qiao, C.-S. Li, and K.-T. Chao, Phys. Rev. D **54**, 5606 (1996).

[12] C.-H. Chang, J.-X. Wang, and X.-G. Wu, Phys. Rev. D **77**, 014022 (2008).

[13] X.-G. Wu, Phys. Lett. B **671**, 318 (2009).

[14] G. T. Bodwin, E. Braaten, and G. P. Lepage, Phys. Rev. D **51**, 1125 (1995).

[15] Y.-J. Zhang, Y.-J. Gao, and K.-T. Chao, Phys. Rev. Lett. **96**, 092001 (2006).

[16] T. Hahn, Comput. Phys. Commun. **140**, 418 (2001).

[17] R. Mertig, M. Böhm, and A. Denner, Comput. Phys. Commun. **64**, 345 (1991).

[18] T. Hahn and M. Perez-Victoria, Comput. Phys. Commun. **118**, 153 (1999).

[19] E. J. Eichten and C. Quigg, Phys. Rev. D **52**, 1726 (1995).